Dynamic and Spectroscopic Studies of Single Molecules Physisorbed on Graphite Substrates. 2. Application to the Ammonia Molecule

A. Lakhlifi*,† and J. P. Killingbeck‡

Laboratoire d'Astrophysique de l'Observatoire de Besançon, Université de Franche−Comté, UMR CNRS 6091, 41 bis Avenue de l'Observatoire, BP 1615, 25010 Besançon Cedex, France, and Mathematics Department, University of Hull, Hull HU6 7RX, United Kingdom

Received: December 16, 2004; In Final Form: April 5, 2005

In the present paper, the theoretical approach developed in paper 1 is applied to an NH_3 molecule adsorbed on a graphite substrate. The potential energy surfaces (PESs) for the interaction between the molecule and the graphite crystal are described in detail. The molecule exhibits two quasi-equivalent angular position minima of energy ("up" and "down") along the perpendicular axis to the surface. The PES calculations also indicate that the NH_3 molecule has a rotational motion that is moderately hindered, with an energy barrier value of about 14 meV and also a quasi-free lateral translational motion above the surface, indicating a weak corrugation of the graphite (0001) surface. The isosteric heat of adsorption is calculated and is in agreement with the experimental one. Finally, the infrared absorption spectra for the vibrational mode frequency regions are obtained.

I. Introduction

It is widely accepted by the astrophysics community that in the universe the dominant mechanism for the formation of H_2 molecules and of a variety of other molecules such as CO, CO_2, HCN, NH_3, CH_4, and CH_3OH (as well as more complex ones)[2] is the action of surface-catalyzed chemical reactions on low-temperature dust grains. The presence of all of these components in the interstellar medium has been revealed by observations in the infrared frequency regions.

The cold interstellar medium is characterized by its high density of atoms and molecules ($n \gtrsim 10^3$ cm^{-3}) and its low temperature of about 10−20 K. Current knowledge of interstellar dust grains indicates that they have both a silicate and a carbonaceous composition.

The silicate grains seem to be typically composed of forsterite (Mg_2SiO_4 (100)) material, with alternating planes of MgO and SiO_2, terminating with an MgO one.[1,3] However, in the observed interstellar extinction the feature at 2175 Å is attributed to carbon grains, which may be in the form of graphite, diamond, or amorphous structures[4,6] and may also be in the form of flat polycyclic aromatic hydrocarbons (PAHs).

The graphite (0001) surface is frequently used as a substrate for modeling the interstellar grains to study the dynamics of H_2 formation and to determine the structural and thermodynamic properties (including their temperature dependence) for mono- and multilayer films of atomic and molecular species such as K, N_2, CO_2, NH_3, C_2H_4, the noble gases, and other types of molecules.[7−17]

Recently, many observations have been made in the infrared spectral regions, in a search for ammonia molecules and other molecules in the dust clouds. The abundance of NH_3 in a variety of interstellar objects has been found to be ∼5−30% relative to water ice.[18−21,23] Such observations should provide information that allows us to understand the chemical and physical processes occurring in the interstellar medium. The ammonia molecule is of particular interest since its vibration−inversion mode in the infrared spectral region represents an interesting case that is amenable to theoretical treatment.

The ammonia molecule can, of course, be associated with several different substrates. Although we treat the particular case of a graphite substrate, we note that our approach is more generally applicable. The general principle demonstrated is that by calculating the potential due to the particular subtrate it is possible to use the model of a double-well potential perturbed by changes in the depth or the curvature of the effective potential to explain the environmental effect on the inversion spectrum. A numerical calculation showing the extreme sensitivity of a double-well potential function to a perturbing potential was given long ago;[22] in particular it showed how an odd parity potential could suppress the inversion motion.

During the 1980s, we developed theoretical models to describe ammonia molecules trapped in rare gas (Ar, Kr, Xe) and in nitrogen matrixes at low temperatures[24−29] with the aim of interpreting the available experimental infrared spectra.

In these studies, we made detailed calculations of the potential energy surfaces needed to describe the statics and dynamics of the different degrees of freedom and their couplings. The behavior of the inversion motion in the different systems was investigated in detail. Because of the symmetry of the trapping sites, the double-well potential function associated with the vibration−inversion ν_2 mode remains symmetric, but its barrier height increases with respect to that for the gas phase. The splittings of the first two vibration levels are accordingly decreased.

We have recently studied the adsorption of an ammonia molecule on MgO and NaCl dielectric substrates.[30,31] In these cases, the ν_2 mode is strongly perturbed and shifted toward the blue. In effect, one of the two wells of the potential energy function disappears, and the inversion motion is then forbidden.

* Author to whom correspondence should be addressed. E-mail: azzedine.lakhlifi@obs-besancon.fr.
† Université de Franche−Comté.
‡ University of Hull.

10.1021/jp0442706 CCC: $30.25
Published on Web 05/14/2005

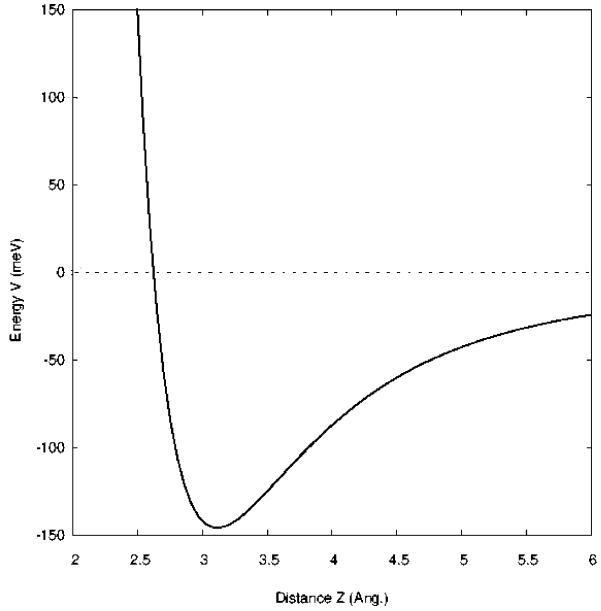

Figure 1. Potential energy V_{MG} as a function of the Z coordinate of the center of mass of the ammonia molecule perpendicular to the surface of the graphite substrate.

We have studied the adsorption of an ammonia molecule on the surface of an argon cluster at low temperatures.[32] Although the double-well potential energy function acquires only a weak asymmetry, the inversion motion of the vibrational ground state is forbidden, so that the molecule cannot pass from one potential well to the other. In all of these cases, the calculated spectra were in agreement with the experimental ones.

In the present work, we apply the theoretical approach presented in paper 1 to the case of the ammonia monomer adsorbed on a graphite (0001) surface, to predict its infrared spectra. Section II describes the adsorbate−substrate system and the interaction potential model to be used in our calculations. In section III, the total Hamiltonian associated with the optical modes is treated, using the renormalization method to separate the different motions from each other. The frequency shifts of the ν_1, ν_2, ν_3, and ν_4 vibrational modes and the orientational level scheme are then calculated, and the surface effect on the NH_3 inversion motion is treated in detail. Finally, sections IV and V are devoted to the construction of the infrared profile spectra and to a discussion of the improvements that could be made to the model to take into account all of the coupling terms that determine the inhomogeneous widths of the line shapes.

II. Ammonia−Graphite Interaction Model

A. Molecule−Graphite System. The ammonia molecule is an oblate symmetric top that possesses a 3-fold symmetry axis. Because of its inversion motion (umbrella mode), its rotational levels are split; the associated infrared spectra can thus give interesting information about the perturbative environment of the molecule.

The graphite crystal is extensively used as a model to simulate the behavior of interstellar grains in studies of the physical and chemical phenomena of adsorbed molecular species. In effect, experimentally detected absorption features of carbon grains were attributed to the presence of small spherical graphite crystals of size ∼200 Å in the dust clouds.[4,6]

In this work, we consider an ammonia molecule adsorbed on a graphite basal plane (0001) at low temperatures (Figure 1 of paper 1). To reduce the required numerical calculation times, our graphite crystal will be constituted of 10 planes with radii ∼35 Å; this does not influence the interaction potential energy surfaces between the molecule and the substrate.

B. Interaction Potential Energy. As we have seen in paper 1, the interaction potential energy V_{MG} between the adsorbed ammonia molecule and the graphite substrate can be written as

$$V_{MG} = V_{LJ} + V_E + V_I \tag{1}$$

where V_{LJ}, V_E, and V_I characterize the quantum, electrostatic, and induction contributions

$$V_{LJ} = \sum_j \sum_{i=1}^{4} 4\epsilon_{ij}\left\{\left(\frac{\sigma_{ij}}{|\mathbf{r}_{ij}|}\right)^{12}\left[1+\gamma_R\left(1-\frac{6}{5}\cos^2\theta_{ij}\right)\right] - \left(\frac{\sigma_{ij}}{|\mathbf{r}_{ij}|}\right)^{6}\left[1+\gamma_A\left(1-\frac{3}{2}\cos^2\theta_{ij}\right)\right]\right\} \tag{2}$$

$$V_E = \sum_j \mu\cdot\nabla\Phi^j(\mathbf{r}_0) + \frac{1}{3}\sum_j \Theta:\ \nabla\nabla\Phi^j(\mathbf{r}_0) + \cdots \tag{3}$$

and

$$V_I = -\frac{1}{2}\sum_j [\nabla\Phi^M(\mathbf{r}_j):\ \alpha^c:\ \nabla\Phi^M(\mathbf{r}_j)] - \frac{1}{2}\sum_{jj'}[\nabla\Phi^j(\mathbf{r}_0):\ \alpha:\ \nabla\Phi^{j'}(\mathbf{r}_0)] \tag{4}$$

In these expressions, i and j characterize, respectively, the nitrogen and hydrogen atoms of the molecule and the carbon atoms of the graphite substrate. The quantities $\mathbf{r}_{ij}$, ϵ_{ij}, σ_{ij}, θ_{ij}, γ_R and γ_A in eq 2 and the electrical potentials Φ^M and Φ^j of eqs 3 and 4 have been defined in paper 1. We recall that the latter explicitly depends on the quadrupole moment tensor Θ^c of the graphite atoms[33] and on the screening factor L_p of the graphite substrate ($L_1 = 1$ for the surface plane and $L_p = 2/(\epsilon + 1)$ for the internal planes).

The elements of the polarizability α^c and quadrupole moment Θ^c tensors of the graphite atoms are given in the absolute frame (**X,Y,Z**) by

$$\alpha^c_{XX} = \alpha^c_{YY} = \alpha^c_{\perp} \quad \alpha^c_{ZZ} = \alpha^c_{\parallel}$$

$$-2\Theta^c_{XX} = -2\Theta^c_{YY} = \Theta^c_{ZZ} = \Theta^c \tag{5}$$

with all other elements being zero. The elements of the molecular polarizability α, dipole moment μ, and quadrupole moment Θ tensors are given in its tied frame (**x,y,z**) as

$$\alpha_{xx} = \alpha_{yy} = \alpha_{\perp} \quad \alpha_{zz} = \alpha_{\parallel}$$

$$\mu_z = \mu$$

$$-2\Theta_{xx} = -2\Theta_{yy} = \Theta_{zz} = \Theta \tag{6}$$

with all other elements being zero.

The various graphite and molecular characteristic values are given in Table 1.

TABLE 1: Important Parameters for Ammonia, Graphite, and Ammonia−Graphite Combinations

ammonia[a]		graphite[b]		combinations[a,b]		
					gr−N	gr−H
q^e (Å)	1.02	L (Å)	3.36	ϵ (cm^{-1})	22.7	18.3
β^e (deg)	68.	a (Å)	2.46	σ (Å)	3.39	2.97
$\alpha_\perp^e$ (Å^3)	2.18	$\alpha_\perp^c$ (Å^3)	1.44	γ_R	−1.05	−0.54
$\alpha_\parallel^e$ (Å^3)	2.42	$\alpha_\parallel^c$ (Å^3)	0.41	γ_A	∼0.4	∼0.4
μ^e (D)	1.48	Θ^c (D Å)	1.0			
Θ^e (D Å)	−2.93	ϵ	2.8			
B^e (cm^{-1})	9.94					
C^e (cm^{-1})	6.31					

[a] From ref 41 and references therein. [b] From refs 8, 14, 15, 42, and 43.

C. Potential Energy Surface. *1. Equilibrium Configuration.* In eq 17 of paper 1, the interaction potential energy V_{MG} was written as

$$V_{MG} = V_{MG}^e(\mathbf{r}_0) + V_{MG}^e(\Omega) + V_{MG}^e(\{Q_\nu\}) + V_{MG}^e(\mathbf{u}(0),\mathbf{u}(\{j\})) + \Delta V_{MG}(\{Q_\nu\},\Omega,\mathbf{u}(0),\mathbf{u}(\{j\})) \quad (7)$$

where $V_{MG}^e(\mathbf{r}_0)$ is the potential energy for the equilibrium configuration of the rigid ammonia molecule adsorbed on the graphite surface and the latter terms describe the dynamical parts, which depend on the internal and external degrees of freedom. Note that the last term ΔV_{MG} represents the dynamic coupling between all of the molecular and all of the substrate degrees of freedom.

The potential energy surface $V_{MG}^e(X,Y)$, which is experienced by the rigid molecule as it moves laterally above the surface, is determined by minimizing V_{MG} with respect to both the perpendicular distance Z between the molecular center of mass and the surface and the angular coordinates (φ,θ,χ). The graphite surface appears to be weakly corrugated around the surface carbon hexagon.

The minimum value of the potential energy surface $V_{MG}^e(X,Y)$ is found to be −146 meV, with the molecule at $Z^e \simeq 3.15$ Å above the hexagon site center. The maximum value is found to be −144 meV, with the molecule at $Z^e \simeq 3.25$ Å above the bridge and atop sites. These values are in good agreement with the value −145 meV, with the molecule at $Z^e \simeq 3.22$ Å, calculated by Crowell.[34]

The molecule also exhibits two almost equally energetic angular equilibrium positions along the perpendicular axis to the surface for $\theta^e = 0$ and $\theta^e = \pi$ (with φ and χ being free motions). The energy difference between these two angular positions is $\lesssim 2$ meV, and they correspond, respectively, to the H atoms "pointing up" and "pointing down" with respect to the surface. The rotational energy barrier between these two positions is equal to 14 meV. Moreover, the variations of the potential energies $V_{MG}^e(Z)$ connected to $\theta^e = 0$ and $\theta^e = \pi$ are quite similar. In Figure 1, we give such a variation for $\theta^e = 0$.

It should be noted that the induction energy contribution due to the polarization of the NH_3 molecule by the quadrupole moments of the graphite atoms (the second term of eq 4) is negligibly small, while the quantum energy contribution V_{LJ} (eq 2) represents more than 80% of the total energy V_{MG}.

2. Isosteric Heat of Adsorption. As a first test of this interaction potential model, the isosteric heat of adsorption of an NH_3 molecule adsorbed on the graphite surface is calculated and is compared with the available experimental data.

Within the rigid molecule and substrate approximation, the isosteric heat of adsorption E_a can be defined as the energy required to keep a molecule with thermal energy $(n/2 + 1)kT$ on the surface of the graphite substrate. E_a is expressed as[35]

$$E_a \simeq \left(\frac{n}{2} + 1\right)kT - V_{MG}^e(\mathbf{r}_0^e) - \sum_{s=1}^{n} \frac{\hbar\omega_s}{2} \coth\left(\frac{\hbar\omega_s}{2kT}\right) \quad (8)$$

where n is the number of degrees of freedom for the molecule and k is the Boltzmann constant. The ω_s values ($s = 1-6$) are the frequencies connected to the translational and angular motions of the molecule, in the harmonic approximation. Note, however, that because of the quasi-free character of the lateral translation (X,Y) and of the precession φ and proper rotation χ motions of the molecule, only the perpendicular translation Z and angular θ motions contribute to the calculation of the adsorption energy. The corresponding frequencies are $\omega_Z \simeq 155$ cm^{-1} and $\omega_\theta \simeq 47$ cm^{-1}.

At a temperature $T = 195$ K, the isosteric heat of adsorption calculated in this work is 178 meV, in agreement with the estimated experimental value of 172 meV given by Avgul and Kiselev.[36] For lower temperatures, the isosteric heats of adsorption E_a are calculated to be 137 meV (at $T = 10$ K) and 143 meV (at $T = 30$ K).

III. Optical Hamiltonian $\tilde{H}_a$

As already described in paper 1, the optically active system is formed by the vibration−orientation modes of the adsorbed molecule and has the Hamiltonian

$$\tilde{H}_a = \tilde{H}_{vib} + \tilde{H}_{orient} \quad (9)$$

where $\tilde{H}_{vib}$ and $\tilde{H}_{orient}$ are, respectively, the renormalized Hamiltonians associated with the vibrational and orientational modes and are treated separately by using the Born−Oppenheimer approximation.

A. Angular Motions. For the rigid ammonia molecule adsorbed on the graphite substrate, the renormalized orientational Hamiltonian $\tilde{H}_{orient}$ is written as

$$\tilde{H}_{orient} = T_{rot} + V_{MG}^e(\Omega) \quad (10)$$

where T_{rot} is the rotational kinetic Hamiltonian for the free (symmetric top) molecule. It is expressed in terms of the orientational degrees of freedom $\Omega = (\varphi,\theta,\chi)$ with respect to the absolute frame as[37]

$$T_{rot} = -B\left\{\frac{\partial^2}{\partial\theta^2} + \cot\theta\frac{\partial}{\partial\theta} + \frac{1}{\sin^2\theta}\frac{\partial^2}{\partial\varphi^2} + \left(\cot^2\theta + \frac{C}{B}\right)\frac{\partial^2}{\partial\chi^2} - 2\frac{\cot\theta}{\sin\theta}\frac{\partial^2}{\partial\varphi\partial\chi}\right\} \quad (11)$$

where B and C are the rotational constants for the motion of the molecular C_3 symmetry axis and the motion around this axis, respectively. Their values for the rigid NH_3 molecule are given in Table 1.

The orientational potential energy surface $V_{MG}^e(\Omega)$ that is experienced by the nonvibrating NH_3 molecule at its adsorption site has been calculated numerically. The associated motion is not a free rotational behavior but rather a moderately hindered angular motion, with an energy barrier of 14 meV, as mentioned above. A Gauss−Legendre integration method allows $V_{MG}^e(\Omega)$

to be described in a basis of $D(\varphi,\theta,\chi)$ Wigner rotation elements,[38] in the form

$$V^{e}_{MG}(\varphi,\theta,\chi) = \sum_{lpq} A^{l}_{p,q} D^{l}_{p,q}(\varphi,\theta,\chi) \tag{12}$$

In this expression, $l = 0, 1, ...$ is an integer number connected to the angle θ, while p and q are connected to the angles φ and χ, respectively, and can take the values $0, \pm1, ..., \pm l$. We note however that, because of the C_{3v} symmetry of the molecule, the number q can only take values that are multiples of 3 (including zero). In eq 12, the $A^{l}_{p,q}$ fitting coefficients are complex numbers that have been calculated up to $l = 8$. The higher expansion terms were negligibly small.

The Schrödinger equation connected to the orientational Hamiltonian $\tilde{H}_{orient}$

$$\tilde{H}_{orient}|\widetilde{jmk}\rangle = E_{\widetilde{jmk}}|\widetilde{jmk}\rangle \tag{13}$$

can now be solved in a basis of the eigenelements E_{JMK} and $|JMK\rangle$ associated with the free rotational motion of the molecule. The eigenvectors $|\widetilde{jmk}\rangle$ are written as linear combinations

$$|\widetilde{jmk}\rangle = \sum_{JMK} \Lambda^{jmk}_{JMK}|JMK\rangle \tag{14}$$

where the Λ values are the resulting coefficients obtained by solving the system of secular equations

$$\sum_{JMK} \Lambda^{jmk}_{JMK} \sum_{J'M'K'} \left\{ (E_{J'M'K'} - E_{j'm'k'})\delta_{J,J'}\delta_{M,M'}\delta_{K,K'} + \left(\frac{2J+1}{2J'+1}\right)^{1/2} \sum_{lpq} A^{l}_{p,q} C(JlJ';MpM') C(JlJ';KqK') \right\} \Lambda^{j'm'k}_{J'M'K'} = 0 \tag{15}$$

where δ and C are the Kronecker symbols and the Clebsch−Gordan coefficients that appear after applying the addition theorem for the $D(\varphi,\theta,\chi)$ elements.[38]

Equation 15 is then solved by diagonalizing the characteristic matrix of minimum dimension 1771×1771, which allows terms in eq 12 up to $l = 8$ to perturb levels up to $j = 0, 1, 2$, with higher jmk levels being negligibly populated at low temperatures ($T \simeq 10-30$ K).

The resulting orientational energy level scheme up to $j = 2$ is presented in Figure 2, with (for comparison) the corresponding free rotational (dashed) levels. It can be seen that the orientational levels exhibit splittings that are due to the lifting of the degeneracy of the magnetic m and spinning k quantum numbers. Moreover, the resulting Λ coefficients indicate that the eigenvectors $|jmk\rangle$ (eq 11) arise from a strong perturbation of the free $|JMK\rangle$ rotational states, as described by the orientational potential energy surface. The calculated eigenvectors will be used to calculate the orientational transition elements for the infrared spectrum.

B. Vibrational Frequency Shifts. The calculated values of the first and second derivatives of the vibration-dependent potential term $V^{e}_{MG}(\{Q_v\})$ (eq 20 of paper 1) are small. They only involve vibrational frequency shifts and splittings, with respect to the gas-phase molecule,[5] which can be calculated by using a first-order perturbation treatment. To this order of perturbation, the vibrational eigenvectors do not change.

For the nondegenerate bond-stretching vibrational mode ν_1 and the doubly degenerate bending-deformation modes ν_3 and ν_4, the calculated values are presented in Table 2. One can show that for the adsorption equilibrium position $\theta^{e} = 0$ of the molecule (with the H atoms pointing up with respect to the surface) the vibrational frequencies of the ν_1 and ν_3 modes are blue-shifted, while the ν_4 one is red-shifted. Moreover, the ν_3 and ν_4 modes exhibit negligibly small degeneracy removals ($\sim$0.1 cm^{-1}) due to the adsorption process.

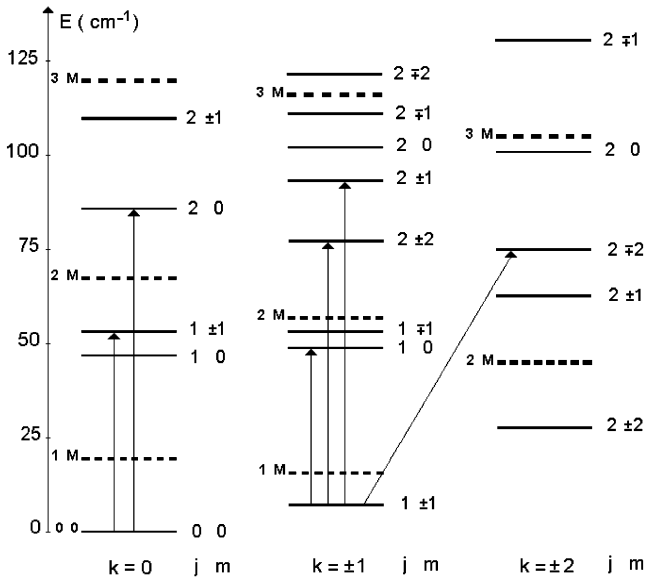

Figure 2. Orientational level scheme of the rigid ammonia molecule adsorbed on the surface of the graphite substrate (solid levels). For comparison, the free rotational level scheme is also given (dashed levels). The arrows show the nonnegligible transitions used in the bar spectrum calculations.

TABLE 2: Vibrational Frequency Shifts of the ν_1, ν_3, and ν_4 Modes of NH_3 Adsorbed on the Graphite Substrate, Together with the Gas-Phase Frequencies

orientational positions	$\theta^{e} = 0$	$\theta^{e} = \pi$	gas-phase frequencies (cm^{-1})
$\Delta\omega_1$	5.5	4.4	3337
$\Delta\omega_3 a$	5.9	3.3	3448
$\Delta\omega_3 b$	5.9	2.4	
$\Delta\omega_4 a$	−2.7	2.2	1627
$\Delta\omega_4 b$	−2.7	0.1	

However, for the position $\theta^{e} = \pi$ of the molecule (with the H atoms pointing down with respect to the surface), the vibrational frequencies of the three modes are blue-shifted, with degeneracy removals (splittings) of $\sim$1 and $\sim$2 cm^{-1}, respectively, for the ν_3 and ν_4 modes.

C. Vibration−Inversion ν_2 Mode. *1. Free NH_3.* In the ν_2 vibration−inversion mode of the free NH_3 molecule (gas-phase state), the hydrogen atoms can pass from one side of the nitrogen atom to the other. This is generally described, to a good approximation, as a one-dimensional tunneling motion of one particle in a symmetrical double-well potential function (left (L) and right (R) wells) with a high, but finite, hindering barrier (254 meV).[39] In Figure 3a, this potential function is shown as a function of the angle between the N−H bond and the plane of the H atoms. The solution of the vibrational problem leads to vibrational energy levels that are split into doublets, + and −. The first four energy levels and their wave functions are also shown in Figure 3a and are then described by $|v_2^{(\alpha)}\rangle$ ($\alpha = +, -$), instead of $|v_2\rangle$. They can be expressed as linear combinations (symmetric and antisymmetric) of the vibrational wave functions $|v_2^{(L)}\rangle$ and $|v_2^{(R)}\rangle$ associated with the left and right wells. The combination coefficients for the fundamental and first excited states are presented in Table 3, and the values of the transition elements $|\langle v_2^{(\alpha)}|Q_2|v_2'^{(\alpha')}\rangle|$ are given in Table 4.

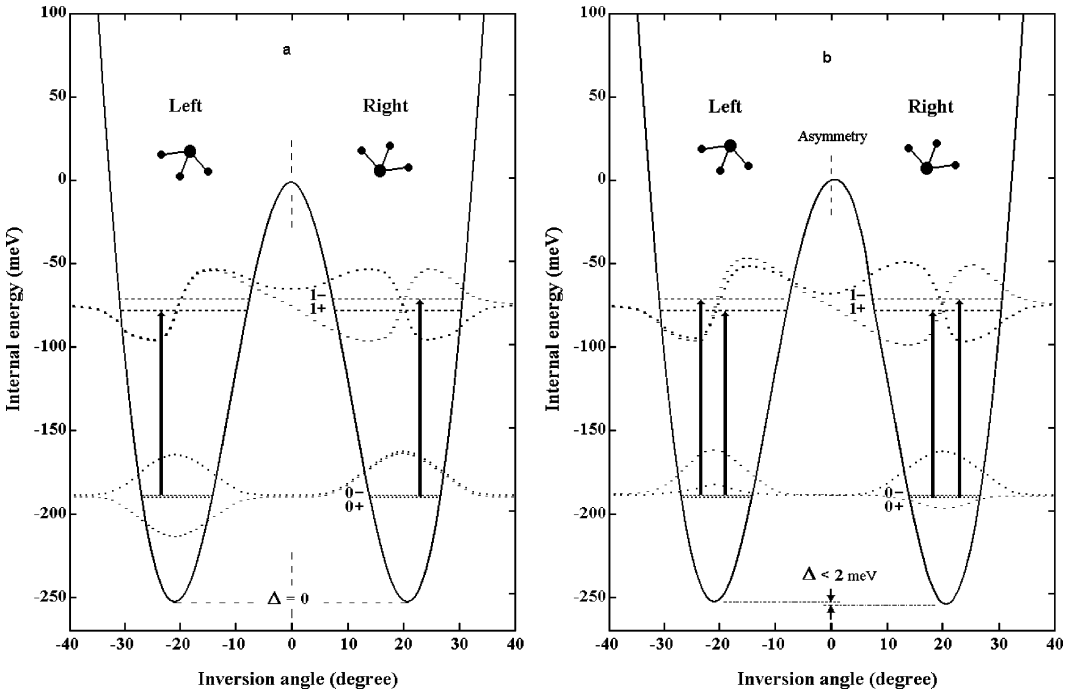

Figure 3. Vibration−inversion double-well potential energy of NH_3 as a function of the angle between the N−H bond and the plane of the H atoms. The obtained energy levels, their associated wave functions, and the allowed transitions are also shown (a) for the gas-phase molecule and (b) for the adsorbed one.

TABLE 3: Linear Combination Coefficients of the $|v_2^{(\alpha)}\rangle$ Vibration−Inversion Wavefunctions in Terms of the $|v_2^{(L)}\rangle$ and $|v_2^{(R)}\rangle$ States Connected to the Left and Right Wells, Respectively[a]

gas NH_3		
$\|v_2^{(\alpha)}\rangle$	$\|v_2^{(L)}\rangle$	$\|v_2^{(R)}\rangle$
$\|0^{(+)}\rangle$	$+1/\sqrt{2}$	$+1/\sqrt{2}$
$\|0^{(-)}\rangle$	$+1/\sqrt{2}$	$-1/\sqrt{2}$
$\|1^{(+)}\rangle$	$+1/\sqrt{2}$	$+1/\sqrt{2}$
$\|1^{(-)}\rangle$	$+1/\sqrt{2}$	$-1/\sqrt{2}$
adsorbed NH_3		
$\|v_2^{(\alpha)}\rangle$	$\|v_2^{(L)}\rangle$	$\|v_2^{(R)}\rangle$
$\|0^{(+)}\rangle$	+0.095	+0.995
$\|0^{(-)}\rangle$	+0.995	−0.095
$\|1^{(+)}\rangle$	+0.683	+0.730
$\|1^{(-)}\rangle$	+0.730	−0.683

[a] The sum of the squares of the coefficients for each state must be equal to 1.

They indicate that in the near-infrared frequency region only the vibration−inversion transitions $|0^{(+)}\rangle \rightarrow |1^{(-)}\rangle$ and $|0^{(-)}\rangle \rightarrow |1^{(+)}\rangle$ are allowed.

2. Adsorbed NH_3. As seen above, when the molecule is adsorbed on the graphite surface, there is an energy difference of $\lesssim 2$ meV between the $\theta^e = 0$ and the $\theta^e = \pi$ adsorption positions, with a rotation barrier of about 14 meV that corresponds to a hindered rotational motion.

In these conditions, the ν_2 vibration−inversion double-well potential function acquires an asymmetric form, with an energy difference $\Delta \lesssim 2$ meV between the two well depths and in addition an increase of $\simeq 4$ meV in the height of the hindering barrier. This potential function is shown in Figure 3b.

The corresponding Schrödinger equation was solved numerically using a discrete variable representation method.[40] The first four energy levels and their associated wave functions are shown in Figure 3b; the resulting eigenvector coefficients and the values

TABLE 4: Averages and Transition Elements (Å) of the Vibration−Inversion Normal Coordinate Q_2 for the Ammonia Molecule in the Gas Phase and When Adsorbed on the Surface of the Graphite Substrate

		gas	adsorbed
$\|v_2^{(\alpha)}\rangle\|$	$\|v_2'^{(\alpha')}\rangle$	$\|\langle v_2'^{(\alpha)}\|Q_2\|v_2'^{(\alpha')}\rangle\|$	$\|\langle v_2^{(\alpha)}\|Q_2\|v_2'^{(\alpha')}\rangle\|$
$\|0^{(+)}\rangle$	$\|0^{(+)}\rangle$	∼0	0.364
	$\|0^{(-)}\rangle$	0.372	0.101
	$\|1^{(+)}\rangle$	∼0	0.053
	$\|1^{(-)}\rangle$	0.081	0.063
$\|0^{(-)}\rangle$	$\|0^{(-)}\rangle$	∼0	0.360
	$\|1^{(+)}\rangle$	0.083	0.064
	$\|1^{(-)}\rangle$	∼0	0.052
$\|1^{(+)}\rangle$	$\|1^{(+)}\rangle$	∼0	0.025
	$\|1^{(-)}\rangle$	0.323	0.323
$\|1^{(-)}\rangle$	$\|1^{(-)}\rangle$	∼0	0.024

of the transition elements are given in Tables 3 and 4, respectively.

Furthermore, Figure 3b shows that in the fundamental vibrational state, there is only a very small probability of tunneling from one well of the potential function to the other.

When the molecule undergoes the near-infrared excitation $\nu_2 = 0 \rightarrow \nu_2 = 1$, the transitions can take place with and/or without inversion motion. In effect, the corresponding transition elements are not zero (Table 4); in contrast to the free molecule case, all four transitions are allowed. Moreover, by introducing the vibration-dependent part $V^e_{MG}(\{Q_\nu\})$ of the potential energy, one can calculate the frequency shifts of these transitions. The resulting values and the squared transition elements are given in Table 5.

D. Dynamic Orientation−Phonon Coupling. As explained in paper 1, within the adiabatic approximation, the dynamic frequency shifts and broadenings of the infrared line transitions depend on the time correlation functions and on the averages of the dynamic orientation−phonon coupling Hamiltonians $\Delta\tilde{H}_1$ and $\Delta\tilde{H}_2$, which correspond to the one- and two-phonon processes, respectively.

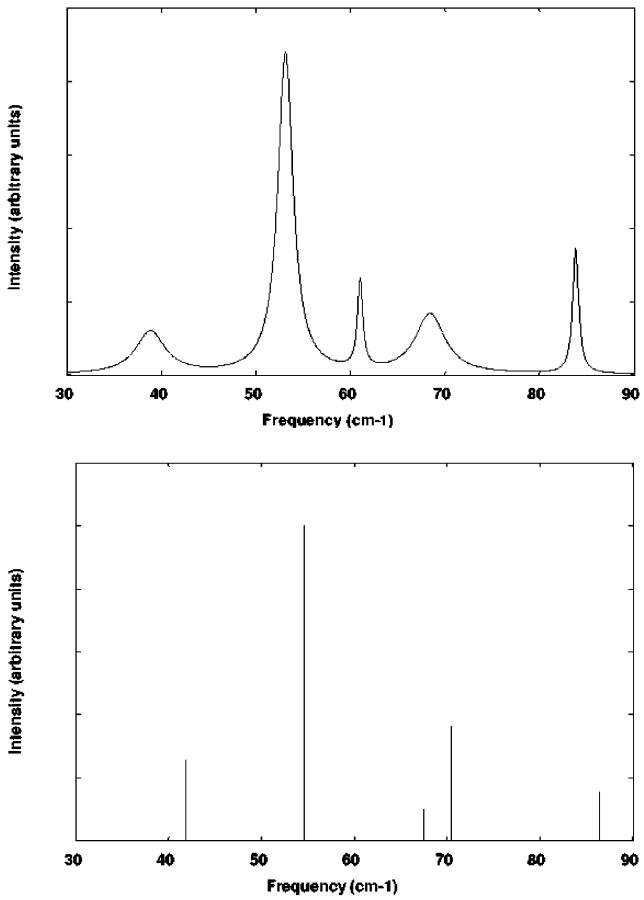

Figure 4. Orientational infrared spectra of the ammonia molecule adsorbed on the surface of the graphite substrate: (lower) bar spectrum and (upper) profile spectrum.

TABLE 5: Vibration−Inversion Frequencies (cm^{-1}), Frequency Shifts (cm^{-1}), and Squared Transition Elements ($Å^2$) of the Normal Coordinate Q_2 for the Ammonia Molecule Adsorbed on the Surface of the Graphite Substrate

$\|0^{(\alpha)}\rangle \rightarrow \|1^{(\alpha')}\rangle$	ω_2	$\Delta\omega_2$	$\|\langle 0^{(\alpha)}\|Q_2\|1^{(\alpha')}\rangle\|^2$
$\|0^{(+)}\rangle \rightarrow \|1^{(+)}\rangle$	942.9	−0.9	2.8×10^{-3}
$\|0^{(+)}\rangle \rightarrow \|1^{(-)}\rangle$	977.4	18.7	4.0×10^{-3}
$\|0^{(-)}\rangle \rightarrow \|1^{(+)}\rangle$	939.8	−5.4	4.2×10^{-3}
$\|0^{(-)}\rangle \rightarrow \|1^{(-)}\rangle$	974.3	14.2	2.7×10^{-3}

For the ammonia molecule adsorbed on a graphite substrate, the expressions for $\Delta\tilde{H}_1$ and $\Delta\tilde{H}_2$ are given in Appendix A of this paper. The coefficients given here are the first- and second-order derivatives of the interaction potential energy V_{MG} with respect to the distance between the molecule and the graphite atoms. They decrease rapidly with increasing distance, and thus in our calculations only the interaction potential terms between the molecule and its nearest-neighbor carbon atoms are considered.

IV. Results and Discussion

As shown in section II.C.1, the ammonia molecule adsorbed on the graphite surface has two positions of orientational equilibrium at $\theta^e = 0$ and $\theta^e = \pi$. The total number $\mathcal{N}$ of active molecules can thus be written as $\mathcal{N} = \mathcal{N}^{(0)} + \mathcal{N}^{(\pi)}$.

Also, since the equilibrium energies at 0 and π are almost identical, we can suppose that $\mathcal{N}^{(0)} = \mathcal{N}^{(\pi)} = (1/2)\mathcal{N}$ when calculating the infrared spectra. The spectra corresponding to each vibrational mode show important changes with respect to the corresponding gas-phase spectra.

TABLE 6: Some Relevant Parameters for the Transitions Which Produce the Orientational Bar Spectrum[a]

transition	$jmk \rightarrow j'm'k'$	$\omega_{jmk\rightarrow j'm'k'}$	I_0	$\Delta^{(1)}$	$\Delta^{(2)}$	$\Gamma^{(2)}$
000	→ 000	0	0	0	0	0.1
	→ 1 ± 1 ± 1	7.4	0	−0.5	0.4	0.1
	→ 10 ± 1	49.2	0	−4.2	2.1	1.9
	→ 1 ± 10	54.5	8.5	−3.7	2.3	1.0
	→ 200	86.4	1.3	−5.2	2.6	0.4
1 ± 1 ± 1	→ 000	−7.4	0	0.5	−0.4	0.1
	→ 1 ± 1 ± 1	0	0	0	0	0.1
	→ 2 ± 2 ± 2	21.8	0	−1	1.5	0.1
	→ 10 ± 1	41.8	2.2	−4.7	1.7	1.9
	→ 1 ± 10	47.1	0	−3.2	1.9	1.0
	→ 2 ± 1 ± 2	54.3	0	−5.7	2.2	0.3
	→ 2 ∓ 2 ± 2	67.5	0.8	−8.7	2.2	0.3
	→ 2 ∓ 2 ∓1	70.4	3.1	−4.2	2.2	1.9
2 ± 2 ± 2	→ 1 ± 1 ± 1	−21.8	0	1	−1.5	0.1
	→ 2 ± 2 ± 2	0	0	0	0	0.1

[a] $\omega_{jmk\rightarrow j'm'k'}$ (cm^{-1}) and I_0 (in arbitrary units) are the orientational line frequency and intensity, respectively. $\Delta^{(1)}$ (cm^{-1}) and $\Delta^{(2)}$ (cm^{-1}) are the line shifts discussed in the text, and $\Gamma^{(2)}$ (cm^{-1}) is the line width.

A. Infrared "Bar Spectra". From eqs 52 and 53 of paper 1 and the associated discussion, it follows that when the dynamic coupling between the optically active modes and the bath states is disregarded, then the dynamic line shifts and line widths are supposed to be zero. The term $\Gamma^{(2)}/((\omega - \omega_{\upsilon jmk\rightarrow\upsilon' j'm'k'} - \Delta\omega_{\upsilon\upsilon'} - \Delta^{(1)} - \Delta^{(2)})^2 + (\Gamma^{(2)})^2)$ in eq 52 (and the analogous term in eq 53) is then replaced by the Dirac function $\delta(\omega - \omega_{\upsilon jmk\rightarrow\upsilon' j'm'k'} - \Delta\omega_{\upsilon\upsilon'})$, and one obtains the infrared bar spectra. It should be noted that we denote by $\omega_{\upsilon jmk\rightarrow\upsilon' j'm'k'}$ the frequency associated with the vibration−orientation transition between the states $|\upsilon jmk\rangle$ and $|\upsilon' j'm'k'\rangle$, while $\Delta\omega_{\upsilon\upsilon'}$ denotes the vibrational frequency shift, the calculated values of which are given in Table 2.

1. Far-Infrared Spectrum. In the far-infrared frequency region, only the orientational spectrum is obtained ($\upsilon_\nu = \upsilon'_\nu = 0$). At a temperature $T \simeq 10$ K, the calculated absorption frequency and intensity values of the possible line transitions (Figure 2) are given in Table 64.

2. Near-Infrared Spectra. In the near-infrared frequency regions, the integrated absorption coefficients connected to each of the vibrational modes of the ammonia molecules, which are for the $|0_\nu^{(\theta^e)}\rangle \rightarrow |1_\nu^{(\theta^e)}\rangle$ transitions, are given by

$$I_\nu(\omega) = \frac{8\pi^2}{3hc}\omega \sum_{\theta^e=0,\pi} \mathcal{N}^{(\theta^e)} |\langle 0_\nu^{(\theta^e)}|Q_\nu|1_\nu^{(\theta^e)}\rangle|^2 \sum_{jmkj'm'k'} \frac{e^{-\beta E_{jmk}}}{Z^{(\theta^e)}} \left|\left\langle jmk\left|\frac{\partial\mu_A}{\partial Q_\nu}\right|j'm'k'\right\rangle\right|^2 \delta(\omega - \omega_{0jmk\rightarrow 1j'm'k'} - \Delta\omega_\nu^{(\theta^e\rightarrow\theta^e)}) \quad (16)$$

In the calculations using eq 16, the angular matrix elements of $\partial\mu_A/\partial Q_\nu$ involve the appropriate set of angular coordinates, as set out in eqs A.1 and A.2 of Appendix A of paper 1.

The notation for the Q_ν vibrational matrix element as shown in eq 16 is appropriate for the cases of the modes ν_1, ν_3, and ν_4. For the special case of the ν_2 mode, which involves a vibration or vibration−inversion transition (as explained in section III.C.2), the appropriate Q_ν matrix element is specified in the detailed discussion of the calculations for that transition (and also appears in Table 4). In eq 16, E_{jmk} is the eigenenergy (obtained by solving eq 13) of the initial orientational state, $Z^{(\theta^e)}$ defines the orientation canonical partition function associ-

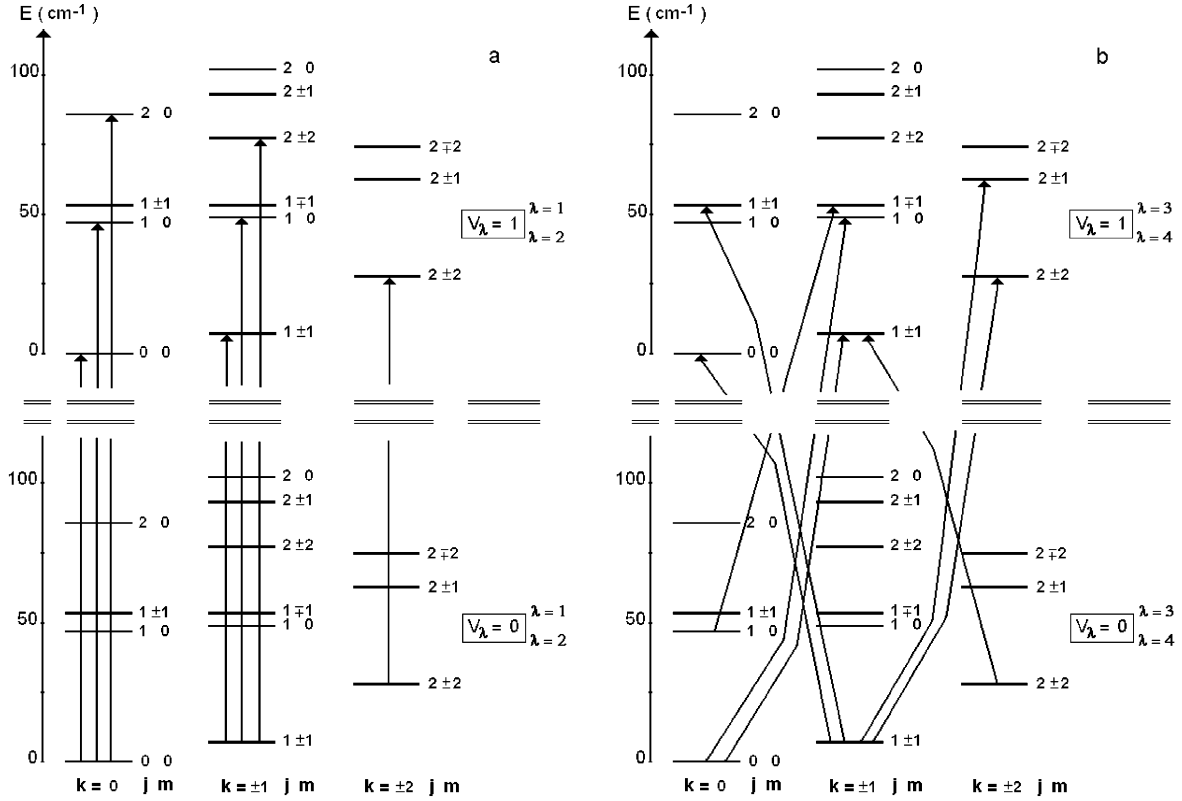

Figure 5. Vibration−orientation transitions of the ammonia molecule adsorbed on the surface of the graphite substrate (a) for ν_1 bond-stretching and ν_2 vibration−inversion symmetric modes and (b) for ν_3 and ν_4 bending-deformation modes.

ated with the fundamental vibrational levels at temperature T, $\beta = (k_B T)^{-1}$, and δ is the Dirac function.

In Figure 5a, we show the vibration−orientation transitions originating from the levels that are populated at 10 K, for the symmetric bond-stretching mode ν_1 and the symmetric vibration−inversion mode ν_2. Figure 5b shows the transitions for the doubly degenerate bending-deformation modes ν_3 and ν_4.

a. Bond-Stretching Mode ν_1. The ν_1 vibrational mode of the NH_3 molecule is symmetric and nondegenerate. When the two equilibrium positions (at 0 and π) are allowed for, the frequency shifts are shown in Table 2. The infrared spectrum is composed of two sets of lines separated by about 1.1 cm^{-1}, as is shown in Figure 6.

In this spectrum, the line pairs at ∼3342 cm^{-1} are due to vibrational transitions only, while those at ∼3384, 3397, and 3412 cm^{-1} correspond to vibration−orientation transitions.

b. Bending-Deformation Modes ν_3 and ν_4. As explained in section III.B, the vibrational frequencies of the ν_3 and ν_4 modes exhibit shifts, with a negligibly small splitting (∼0.1) for the molecules at $\theta^e = 0$. For the molecules at $\theta^e = \pi$ position, the shift is smaller, but the splitting is much larger.

As a result, the infrared vibration−orientation spectrum corresponding to these modes displays three groups of lines separated by 2.6 and 0.9 cm^{-1} for ν_3 and by 2.8 and 2.1 cm^{-1} for ν_4, as is shown in Figures 7 and 8, respectively. Only vibration−orientation transitions are present for the modes ν_3 and ν_4. In effect, the orientational transition elements of these modes depend on the proper rotation angle χ that makes the $\Delta k = 0$ transitions forbidden.

c. Vibration−Inversion ν_2 Mode. The near-infrared spectrum of the ν_2 mode is shown in Figure 9. In this spectrum, the lines at 942.1 and 988.6 cm^{-1} are due to vibrational transitions only, while the more intense lines at 934.5 and 996.2 cm^{-1} are due to vibration−inversion transitions. Moreover, this spectrum exhibits two groups of lines, with the more intense ones at 997.2 and 1043.1 cm^{-1} being due to vibration−orientation transitions

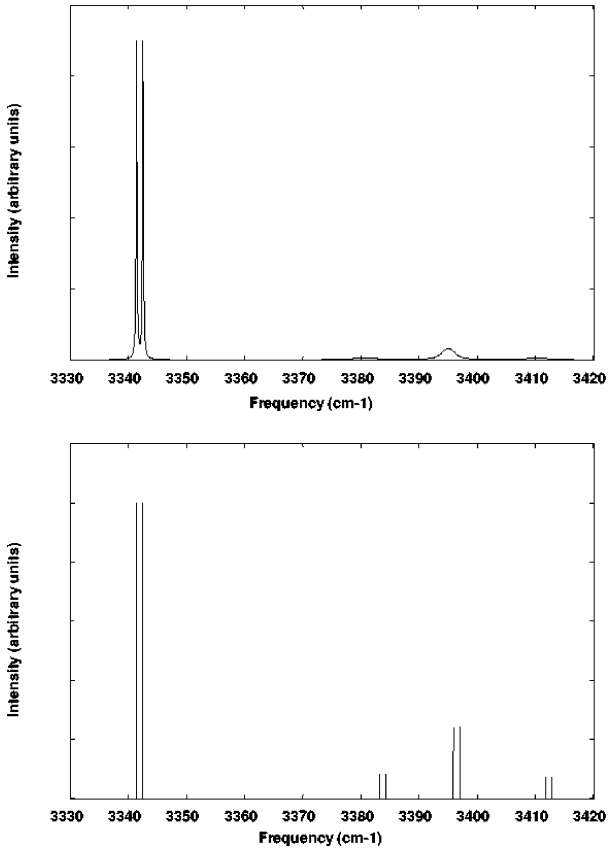

Figure 6. Near-infrared spectra for the ν_1 bond-stretching mode of the adsorbed ammonia molecule: (lower) bar spectrum and (upper) profile spectrum.

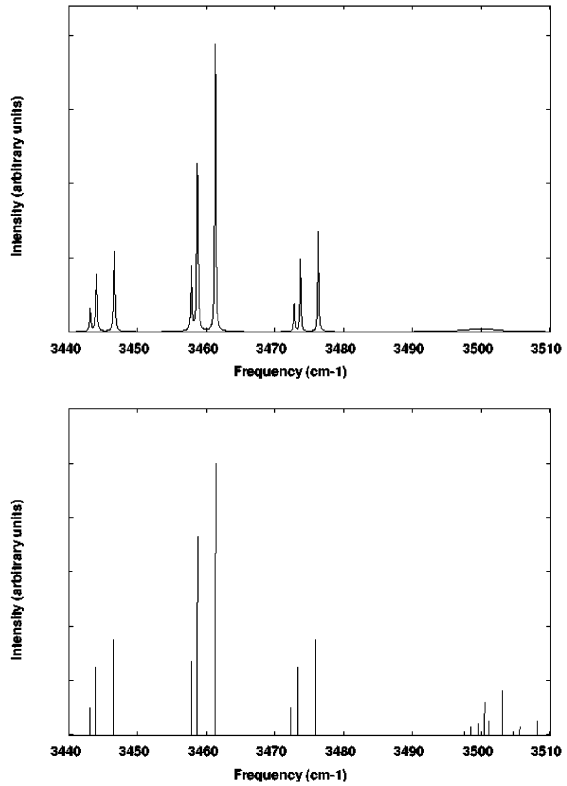

Figure 7. Near-infrared spectra for the ν_3 bending-deformation mode of the adsorbed ammonia molecule: (lower) bar spectrum and (upper) profile spectrum.

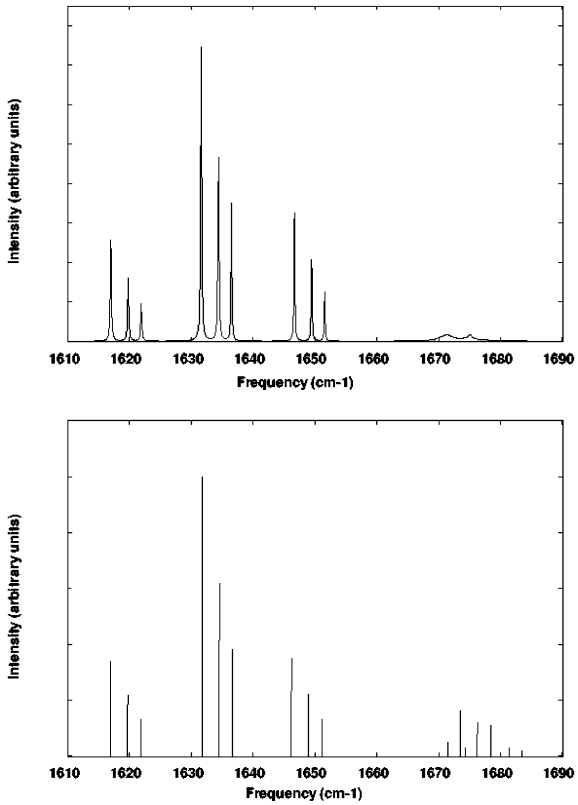

Figure 8. Near-infrared spectra for the ν_4 bending-deformation mode of the adsorbed ammonia molecule: (lower) bar spectrum and (upper) profile spectrum.

and those at 989.5 and 1050.9 cm^{-1} being due to vibration−inversion−orientation transitions.

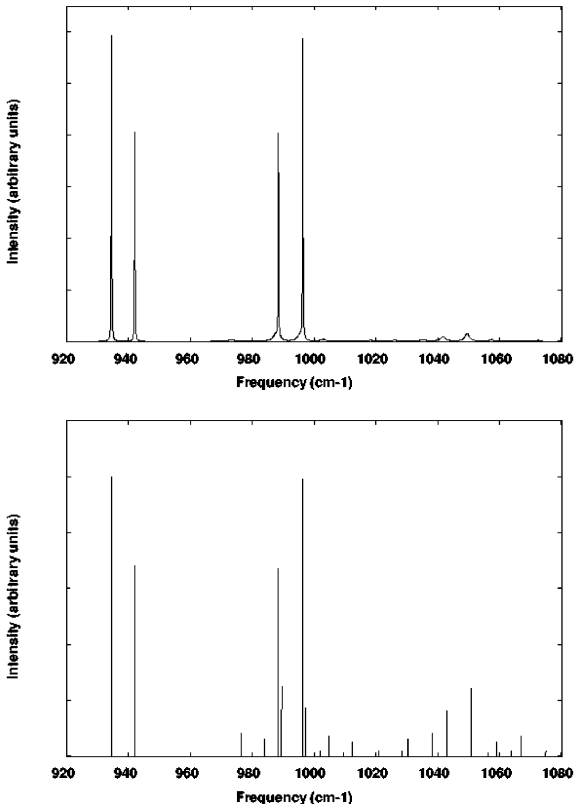

Figure 9. Near-infrared spectrum for the ν_2 vibration−inversion mode of the adsorbed ammonia molecule: (lower) bar spectrum and (upper) profile spectrum.

B. Profile Spectra. Using the dynamic orientation−phonon coupling Hamiltonians $\Delta\tilde{H}_1$ and $\Delta\tilde{H}_2$ given in Appendix A, the line shift $\Delta^{(1)}$ due to the first-order term in the cumulant series expansion of the time evolution operator was calculated as well as the line shift $\Delta^{(2)}$ and line width $\Gamma^{(2)}$ due to the second-order term in the expansion. The various terms appearing in $\Delta^{(1)}$, $\Delta^{(2)}$, and $\Gamma^{(2)}$ are set out in eqs 43−47 of paper 1.

Table 6 shows the calculated $\Delta^{(1)}$, $\Delta^{(2)}$, and $\Gamma^{(2)}$ values at 10 K for lines of nonnegligible intensity that are associated with the vibrational transitions and the vibration−orientation transitions.

The values of $\Delta^{(1)}$, $\Delta^{(2)}$, and $\Gamma^{(2)}$ associated with each line transition in the bar spectrum are inserted into eqs 52 and 53 of paper 1 to yield the profile spectrum.

As explained in the theoretical development of paper 1, $\Delta^{(2)}$ and $\Gamma^{(2)}$ are given by a sum of three types of contributions.

The first and strongest one depends on the vibrational states of the substrate, involving the phonon density via $\omega^2 g(\omega^2)$ for the one-phonon coupling term $\Delta\tilde{H}_1$ and via the product $\omega^2 g(\omega^2)\omega'^2 g(\omega'^2)$ for the two-phonon term coupling $\Delta\tilde{H}_2$. It is also possible to have resonance effects between the phonon frequencies and the orientational transition frequencies $\omega_{jmk\rightarrow j'm'k'}$.

The second contribution depends on the motion of the center of mass of the molecule via the term $\omega_k^2\delta(\omega^2 - \omega_k^2)$ for the one-phonon coupling and via the product $\omega_k^2\delta(\omega^2 - \omega_k^2)$ $\omega_{k'}^2\delta(\omega'^2 - \omega_{k'}^2)$ for the two-phonon coupling term $\Delta\tilde{H}_2$, where k and k' represent the coordinates X, Y, and Z. These contributions only exist when there is a resonance between ω_k and/or $\omega_{K'}$ and $\omega_{jmk\rightarrow j'm'k'}$. For the ammonia molecule, these terms are zero and so do not contribute to the width $\Gamma^{(2)}$; their contribution to $\Delta^{(2)}$ is also very small.

The third type of term couples the molecular motion to that of the substrate via the product $\omega_k^2\delta(\omega^2 - \omega_k^2)\omega^2 g(\omega^2)$. We

note that in this case only the two-phonon coupling $\Delta\tilde{H}_2$ is involved. The contribution to $\Gamma^{(2)}$ is negligible ($\lesssim 0.01$ cm^{-1}), while that to $\Delta^{(2)}$ is larger ($\lesssim 0.3$ cm^{-1}).

We note that $\Delta^{(1)}$ does not depend on the transition frequency $\omega_{jmk\rightarrow j'm'k'}$. Resonances between this frequency and the molecular translational movement thus do not appear in the calculation of $\Delta^{(1)}$; nevertheless there is a nonnegligible contribution from this translation−orientational coupling.

The results of Table 6 show clearly how the small contamination of the lowest orientational levels (000, $1 \pm 1 \pm 1$, and $2 \pm 2 \pm 2$) by the other levels means that the line transitions between these levels have relatively small widths (~ 0.1 cm^{-1}). The infrared profile spectra are shown in Figure 4 and in Figures 6−9.

V. Conclusion

The present calculations use a particular model to study the adsorption processes of the ammonia monomer on the surface of a graphite substrate. To describe the interaction between the molecule and the substrate, a semiempirical atom−atom potential energy surface is used.

Moreover, in the orientational level schemes displayed in Figure 5, additional level shifts and splittings can occur, depending on the υ_ν vibrational state of the molecules. In effect, the potential energy surface $V_M(\varphi,\theta,\chi)$ and the rotational constants B and C of ammonia molecules depend parametrically on the vibrational state, and therefore eq 15 must be solved for both the fundamental ($\upsilon_\nu = 0$) and first excited ($\upsilon_\nu = 1$) states. As a consequence, the line frequency positions in the near-infrared spectra should be slightly shifted with respect to those given in Figures 6−9; in particular the component lines of the pure vibrational bands will not both occur at the same frequency values.

Acknowledgment. Fruitful discussions with Professor G. Jolicard and Dr. D. Viennot are gratefully acknowledged.

Appendix A: Dynamic Orientation−Phonon Coupling Hamiltonians

In the harmonic description of the dynamic translation (molecular center of mass motions + substrate atom vibrations) motions, the expressions of the coupling Hamiltonians $\Delta\tilde{H}_1$ (orientation, one-phonon) and $\Delta\tilde{H}_2$ (orientation, two-phonon) are

$$\Delta\tilde{H}_1 \simeq -500(u(j)-u(0))D_{0,0}{}^1 - 650(u(j)-u(0))D_{0,0}{}^2 - 60u(j)[(D_{-1,0}{}^1 - D_{1,0}{}^1) - i(D_{-1,0}{}^1 + D_{1,0}{}^1)] - 1030u(j)[(D_{-1,0}{}^2 - D_{1,0}{}^2) - i(D_{-1,0}{}^2 + D_{1,0}{}^2)] \quad \text{(A1)}$$

and

$$\Delta\tilde{H}_2 \simeq -2800(u^2(j)+u^2(0))D_{0,0}{}^1 - 3800(u^2(j)+u^2(0))D_{0,0}{}^2 - 430u^2(j)[(D_{-1,0}{}^1 - D_{1,0}{}^1) - i(D_{-1,0}{}^1 + D_{1,0}{}^1)] - 900u^2(j)[(D_{-1,0}{}^2 - D_{1,0}{}^2) - i(D_{-1,0}{}^2 + D_{1,0}{}^2)] \quad \text{(A2)}$$

where $u(0)$ and $u(j)$ represent the dynamic displacements of the molecule and of the carbon atoms from their equilibrium positions, respectively, and the $D^l_{p,m}(\varphi,\theta,\chi)$ functions are the usual rotational matrix elements.[38] Note that the numerical values in the above expressions are given in cm^{-1} Å^{-1} in eq A1 and in cm^{-1} Å^{-2} in eq A2.

Appendix B: Vibrational Dependence of the Molecular Dipole Moment

To determine the infrared absorption coefficient for the ammonia molecule, its dipole moment μ must be developed in a series expansion (at the first order) with respect to the molecular frame (**x,y,z**) in terms of the vibrational normal coordinates Q (eq 15 of paper 1).

$$\mu = \mu^e + \sum_\nu \mathbf{b}^\nu Q_\nu \quad \text{(B1)}$$

where $\mu^e = 1.48$ D and b^ν values are given (in D Å $^{-1}$) as

$$\left\{\begin{array}{ll} b^1 = \dfrac{\partial\mu_z}{\partial Q_1} = 1.404 & b^2 = \dfrac{\partial\mu_z}{\partial Q_2} = -4.409 \\ b^{3a} = \dfrac{\partial\mu_x}{\partial Q_{3a}} = -4.012 & b^{3b} = \dfrac{\partial\mu_y}{\partial Q_{3b}} = 2.465 \\ b^{4a} = \dfrac{\partial\mu_x}{\partial Q_{4a}} = 1.984 & b^{4b} = \dfrac{\partial\mu_y}{\partial Q_{4b}} = -2.559 \end{array}\right\} \quad \text{(B2)}$$

References and Notes

(1) Tielens, A. G. G. M.; Allamandola, L. J. *Composition, Structure, and Chemistry of Interstellar Dust*; NASA Ames Research Center: Moffett Field, CA, 1986. *Interstellar Processes*; Astrophysics and Space Science Library 134; Hollenbach, D. J., Thronson, H. A., Jr., Eds.; Reidel Publishing Company: Newell, MA, 1987.
(2) Verschuur, G. L. *Sky Telesc.* **1992**, *83*, 379.
(3) Watson, G. W.; Oliver, P. M.; Parker, S. C. *Phys. Chem. Miner.* **1997**, *25*, 70.
(4) Draine, B. T. *Astrophys. J.* **1988**, *333*, 848.
(5) Martin, J. M. L.; Lee, T. J.; Taylor, P. R. *J. Chem. Phys.* **1992**, *97*, 8361.
(6) Mathis, J. S.; Whiffen, G. *Astrophys. J.* **1989**, *341*, 808.
(7) Bruch, L. W. *J. Chem. Phys.* **1983**, *79*, 3148.
(8) Vidali, G.; Cole, M. W. *Phys. Rev. B* **1984**, *29*, 6736.
(9) Moller, M. A.; Klein, M. L. *J. Chem. Phys.* **1989**, *90*, 1960.
(10) Roosevelt, S. E.; Bruch, L. W. *Phys. Rev. B* **1990**, *41*, 12236.
(11) Cheng, A.; Steele, W. A. *J. Chem. Phys.* **1990**, *92*, 3858.
(12) Cheng, A.; Steele, W. A. *J. Chem. Phys.* **1990**, *92*, 3867.
(13) Rowntree, P.; Scoles, G.; Xu, J. *J. Chem. Phys.* **1990**, *92*, 3853.
(14) Hansen, F. Y.; Bruch, L. W.; Roosevelt, S. E. *Phys. Rev. B* **1992**, *45*, 11238.
(15) Hansen, F. Y.; Bruch, L. W. *Phys. Rev. B* **1995**, *51*, 2515.
(16) Osterlund, L.; Chakarov, D. V.; Kasemo, B. *Surf. Sci.* **1999**, *420*, 174.
(17) Lou, L.; Osterlund, L.; Hellsing, B. *J. Chem. Phys.* **2000**, *112*, 4788.
(18) Whittet, D. C. B.; Smith, R. G.; Adamson, A. J.; Aitken, D. K.; Chiar, J. E.; Kerr, T. H.; Roche, P. F.; Smith, C. H.; Wright, C. M. *Astrophys. J.* **1996**, *458*, 363.
(19) Lacy, J. H.; Faraji, H.; Sandford, S. A.; Allamandola, L. J. *Astrophys. J. Lett.* **1998**, *501*, 105.
(20) Chiar, J. E.; Tielens, A. G. G. M.; Whittet, D. C. B.; Schutte, W. A.; Boogert, A. C. A.; Lutz, D.; van Dishoeck, E. F.; Bernstein, M. P. *Astrophys. J.* **2000**, *537*, 749.
(21) Dartois, E.; d'Hendecourt, L. *Astron. Astrophys.* **2001**, *365*, 144.
(22) Killingbeck, J. *J. Phys. A* **1988**, 3399.
(23) Gibb, E. L.; Whittet, D. C. B.; Chiar, J. E. *Astrophys. J.* **2001**, *558*, 702.
(24) Girardet, C.; Lakhlifi, A. *J. Chem. Phys.* **1985**, *83*, 5506.
(25) Lakhlifi, A.; Girardet, C. *J. Mol. Spectrosc.* **1986**, *116*, 33.
(26) Girardet, C.; Lakhlifi, A. *Chem. Phys.* **1986**, *110*, 447.
(27) Lakhlifi, A.; Girardet, C. *J. Chem. Phys.* **1987**, *87*, 4559.
(28) Girardet, C.; Lakhlifi, A. *J. Chem. Phys.* **1989**, *91*, 1423.
(29) Girardet, C.; Lakhlifi, A. *J. Chem. Phys.* **1989**, *91*, 2172.
(30) Lakhlifi, A.; Picaud, S.; Girardet, C.; Allouche, A. *Chem. Phys.* **1995**, *201*, 73.

(31) Lakhlifi, A.; Girardet, C. *J. Chem. Phys.* **1996**, *105*, 2471.
(32) Lakhlifi, A. *Eur. Phys. J. D* **2000**, *8*, 211.
(33) Vernov, A.; Steele, W. A. *Langmuir* **1992**, *8*, 155.
(34) Crowell, A. D. *J. Chem. Phys.* **1968**, *49*, 892.
(35) Lakhlifi, A. *Mol. Phys.* **1993**, *78*, 659.
(36) Avgul, N. N.; Kiselev, A. V. *Chem. Phys. Carbon* **1970**, *6*, 1.
(37) Townes, C. H.; Schawlow, A. L. *Microwave Spectroscopy*; McGraw-Hill: London, 1955.
(38) Rose, M. E. *Elementary Theory of Angular Momentum*; Wiley: New York, 1967.
(39) Swalen, J. D.; Ibers, J. A. *J. Chem. Phys.* **1962**, *36*, 1914.
(40) Light, J. C.; Hamilton, I. P.; Lill, J. V. *J. Chem. Phys.* **1985**, *82*, 1400.
(41) Lakhlifi, A.; Girardet, C. *J. Mol. Struct.* **1984**, *110*, 73.
(42) Carlos, W. E.; Cole, M. W. *Surf. Sci.* **1982**, *119*, 21.
(43) Ionov, S. I.; LaVilla, M. E. *J. Chem. Phys.* **1992**, *97*, 9379.